

Caltech Faint Galaxy Redshift Survey XIV: Galaxy Morphology in the HDF (North) and its Flanking Fields to $z = 1.2$ ¹

Sidney van den Bergh², Judith G. Cohen³, David W. Hogg^{4,5,6} and Roger Blandford⁴

ABSTRACT

Morphological classifications are reported for Hubble Space Telescope (HST) images of 241 galaxies in the Hubble Deep Field (HDF) and its Flanking Fields (FF) with measured redshifts in the interval $0.25 < z < 1.2$, drawn from a magnitude-limited redshift survey to $R = 24.0$. The galaxies are divided into three groups with redshifts in the intervals $[0.25, 0.6]$, $[0.6, 0.8]$, $[0.8, 1.2]$. R_{606} images from the first group and I_{814} images from the second and third groups are compared with B-band images of nearby galaxies. All classifications were therefore made at approximately the same rest wavelength. Selection biases are discussed.

We corroborate and extend the results of earlier investigations by observing that:

- Most intermediate and late-type galaxies with $z \gtrsim 0.5$ have morphologies that are dramatically different from those of local galaxies and cannot be shoehorned into the Hubble “tuning fork” classification scheme.
- Grand-design spirals appear to be rare or absent for $z \gtrsim 0.3$.
- Many Sa and Sb spirals with $z \gtrsim 0.6$ do not exhibit well-defined spiral arms. The arms of distant Sc galaxies appear more chaotic than those of their nearby counterparts.
- The fraction of all galaxies that are of types Sc and Scd drops from 23% at $z \sim 0$ to 5% for $z > 0.6$.
- Barred spirals are extremely rare for $z \gtrsim 0.5$.
- Roughly one in five galaxies with $z \gtrsim 0.8$ are compact objects that resemble local E, S0 or Sa galaxies.

¹Based in part on observations obtained at the W.M. Keck Observatory, which is operated jointly by the California Institute of Technology and the University of California

²Dominion Astrophysical Observatory, National Research Council, 5071 West Saanich Road, Victoria, British Columbia, V9E 2E7, Canada: sidney.vandenbergh@nrc.ca

³Palomar Observatory, Mail Stop 105-24, California Institute of Technology, Pasadena, CA 91125 jlc@astro.caltech.edu

⁴Theoretical Astrophysics, California Institute of Technology, Mail Stop 130-33, Pasadena, CA 91125 rdb@tapir.caltech.edu

⁵Current Address: Institute for Advanced Study, Olden Lane, Princeton, NJ 08540 hogg@ias.edu

⁶Hubble Fellow

- Peculiar galaxies are more common beyond $z = 0.3$, especially among late-type spirals, than they are at $z \sim 0$.
- Merging galaxies, particularly those with three or more components, also become more common with increasing redshift.

On the basis of these and similar observations, it is inferred that the development of pronounced spiral structure was delayed until ~ 5 Gyr and that most bulges are probably not formed by disintegrating bars. Major morphological changes were still taking place only ~ 5 Gyr ago even though changes in the integrated light of most galaxies were then much slower than they were ~ 10 Gyr ago.

Subject headings: galaxies: evolution, galaxies: formation, surveys

1. Introduction

The Hubble Space Telescope has, for the first time, allowed us to observe directly the evolution of galaxy morphology over a significant fraction of the age of the Universe. Soon after the images of the Hubble Deep Field North, HDF, and its Flanking Fields (FF) became available (Williams *et al.* 1996, Ferguson, Dickinson & Williams 2000) it was clear that distant and young field galaxies were very different from their local, contemporary counterparts (Abraham *et al.* 1996a,b). Indeed, half a lifetime of experience in galaxy classification (van den Bergh 1998) proved to be of only marginal usefulness in attempts to classify galaxies at intermediate and large look-back times. In the words of Ames (1997), “You are living in a land you no longer recognize. You don’t know the language.” More specifically, it was concluded that “The fraction of interacting and merging objects is seen to be significantly higher in the Hubble Deep Field than it is among nearby galaxies. Barred spirals are essentially absent from the deep sample. The fraction of early-type galaxies in the Hubble Deep Field is similar to the fraction of early-types in the Shapley-Ames Catalog, but the fraction of galaxies resembling archetypal grand-design late-type spiral galaxies is dramatically lower in the distant HDF sample.” (van den Bergh *et al.* 1996). Because no redshifts were available, it was not possible to establish a timescale for galaxy evolution. It is the purpose of the present paper to re-examine these conclusions, using the HDF and FF images and the new redshift information (Cohen *et al.* 2000 and references therein), and to discuss the galaxy evolutionary timescale.

The initial reactions to the HDF images have been largely vindicated and significantly developed over the past four years. (See Abraham 1999, 2000 for excellent reviews.) The most complete information so far available on the morphological evolution of galaxies with $z \lesssim 1$ is by Brinchmann *et al.* (1998) who classified HST images of a complete sample of 341 galaxies, selected from both the CFRS and LDSS surveys, for which ground-based redshifts were available. They found a substantial increase in the fraction of irregular galaxies from $\sim 9\%$ at $z \sim 0.4$ to $\sim 32\%$ at

$z \sim 0.8$ and associated these galaxies with the increase in blue luminosity density with redshift. However, the reliability of this conclusion is undermined by the fact that the standard “irregular” galaxy that Brinchmann *et al.* use to calibrate their classifications appears to be an Sb pec galaxy with a central bulge and the kind of under-developed spiral structure that is typically seen in spirals at large redshift.

Using the same sample, Lilly *et al.* (1998) found that the sizes of large galaxy disks do not change significantly out to $z \sim 1$, but that the rate of star formation was elevated by a factor 3 at $z \sim 0.7$. In a new approach, Abraham *et al.* (1999a) related the evolution of galaxy morphology to their internal star formation as monitored by their spatially-resolved colors. They confirmed that spiral bulges pre-date their disks and followed different evolutionary histories. In a study that also included the HDF South, Abraham *et al.* (1999b) confirmed that barred spirals were comparatively rare prior to $z \sim 0.5$.

Ellipticals, by contrast, appear to have evolved relatively little in density and luminosity since $z \sim 1$. There is evidence for ongoing and declining star formation although less than 5% of their stars are estimated to have formed over this time (Schade *et al.* 1999). They seem to have formed over an extended interval $1 \lesssim z \lesssim 3$ (Odewahn *et al.* 1996, Driver *et al.* 1998). This is consistent with the work of Corbin *et al.* (2000) who find that 12 out of 111 (11%) of their NICMOS images (in a data sample that extends to photometric redshifts as large as $z = 2.7$) are probably elliptical galaxies.

Turning to irregulars, the HST images of 285 CFRS/LDSS galaxies have been analyzed to derive the evolution of the merger fraction out to $z \sim 1$ (Le Févre *et al.* 2000). Up to 20% of luminous galaxies are found to be in physical pairs (some of which may be projections) at $z \sim 0.8$. A typical L^* galaxy was found to have undergone $\sim 1 - 2$ mergers since $z \sim 1$. However, the “chain” galaxies, first identified by Cowie, Hu & Songaila (1995), appear to be neither edge-on spirals nor merger products (Abraham *et al.* 1999b).

In recent years, there has been a shift away from the traditional, descriptive and, inevitably, somewhat subjective morphological approach towards more quantitative measures of galaxy structure like scale lengths, central concentration, asymmetry, and so on. This is particularly valuable for connecting observations to increasingly sophisticated numerical simulations. However, galaxies are too variegated to be completely described by just a few numbers and we believe that a simple morphological approach will continue to be of value, even at high redshift. After all, the durability of the original Hubble (1936) scheme for nearby galaxies is remarkable given all that we have learned about them since the 1930s.

In this paper we continue to use the traditional morphological classification, despite its manifest inadequacy at high redshift, for three reasons. The first is quite modest, to increase our confidence that galaxies at high redshift are quite different from local galaxies by enlarging the sample size. The second is to determine if there are *any* counterparts to certain local galaxy types at high redshift. For example, if it is believed on dynamical grounds (see §4.1) that grand design

spirals take a minimum of ~ 10 Gyr to grow, then the discovery of just one *bona fide* example at $z \sim 1$ would be highly significant. The third reason is that it is important to determine the chronology of these changes and, in the absence of an adequate high redshift classification, the best approach is to compare with the well-understood local classification scheme and to discover when it starts to fail.

In the following section, we describe our procedure and discuss some possible selection biases. In section 3, we give our empirical conclusions and we conclude with a brief interpretation of their implications for physical theories of galaxy formation.

2. Galaxy Classification

2.1. Morphology Sample

Our sample is based on the redshift survey in the region of the HDF of Cohen *et al.* (2000), which includes 671 objects. This survey is 92% complete with respect to the photometric catalogs of Hogg *et al.* (2000) to $R \leq 24$ in the HDF itself, and also 92% complete to $R \leq 23$ in a region 8 arcmin in diameter centered on the HDF. See Cohen *et al.* (2000) for details of the samples, the number of stars, galaxies, and high redshift ($z > 1.5$) galaxies, AGNs and QSOs in the HDF and in the Flanking Fields.⁷

The sample used for morphology and discussed here is divided into three redshift intervals, $0.25 < z < 0.60$, $0.60 < z < 0.80$ and $0.80 < z < 1.20$. In each interval, the sample contains all available galaxies in the spectroscopic redshift catalog with suitable HST images. Thus the low redshift group contains 49 galaxies of which 43 are drawn from the HDF. Four galaxies are in the PC field of the WFPC2 image and two others are just outside the boundary adopted for the HDF but within the coverage of the HST R image. (There is unfortunately no R HST image of the rest of the area of the Flanking Fields.) Apart from this there is no bias in magnitude, color or location in this subsample. The intermediate redshift group includes 70 galaxies, while the high redshift group includes 120 galaxies. Note that the WFPC2/HST I₈₁₄ images do not cover the entire area of the Flanking Fields, and hence some galaxies within the area of the redshift survey could not be used. The fraction of galaxies drawn from the HDF and from the FF is as would be expected based on the relative areas and the rise in galaxy counts as a function of R magnitude in this magnitude regime.

⁷The assembly of the sample for the present morphological study was carried out before the final version of Cohen *et al.* (2000) was available. A few galaxies (~ 10) whose redshifts were only determined in the late fall of 1999 that are included in Cohen *et al.* (2000) are not included here.

2.2. Biases and selection effects

From a practical point of view, the morphological classification of individual galaxies at $z \sim 1$ presents three distinct challenges beyond similar classifications of nearby systems. The first is that the images used for the classification of nearby galaxies might contain as many as $\sim 10,000$ pixels, whereas those of very distant Hubble Space Telescope (HST) images may contain only ~ 100 pixels and apparent changes in fine scale features may simply be a consequence of resolution. Furthermore, due to longer exposure times the quality of the HDF images is markedly superior to that of the FF images. This may lead to some misinterpretation of the morphologies of the faintest FF galaxies, especially the most compact examples. For example, it is often not possible to distinguish Galactic stars with certainty from compact ellipticals of Hubble types E0 and E1. (All of the objects in the present sample, including those that have morphological classification “star” or “E0/star” are extragalactic, on the basis of their redshifts, though.) The comparative statements below are restricted to those that can be made with confidence on the basis of the poorest images. (We note, in passing, that it is the large dynamic range of CCD detectors makes them particularly suitable for use in galaxy classification, van den Bergh & Pierce 1990).

The second challenge is to correct for band-shifting. Galaxy classification is traditionally performed in the B (440nm) band. We find, (*cf* also Fig. 3 from Ferguson *et al.* 2000) that galaxy morphology varies sufficiently slowly with wavelength that it is adequate to compare R_{606} images from the 0.25-0.60 redshift interval (the shift is exact for $z = 0.38$) and I_{814} for $0.60 < z < 1.20$ (exact for $z = 0.85$) with local samples. In particular, the z dependence of the frequency of barred spirals (§3.2) cannot be attributed to band-shifting, as has sometimes been suggested (e.g. Bunker *et al.* 2000, Eskridge *et al.* 2000). Some small band-shift effects could, however, still be experienced for galaxies that have $1.0 \lesssim z \lesssim 1.2$. In such objects the core/halo ratio might be depressed, and giant stellar associations may appear slightly enhanced, relative to similar structures seen at smaller redshifts.

The third challenge is that, in a magnitude-limited survey, we are comparing more luminous objects at high redshift with less luminous objects at low z . We emphasize that our local comparison sample is not the HDF but the more extensive Shapley-Ames catalog. With respect to the sample of the Revised Shapley-Ames Catalog, the median M_B (rest frame) for the HDF sample is about 0.3 mag fainter than that of the RSA, where the median for the RSA sample is taken from figure 5 of Sandage and Tammann (1981) and has been adjusted to our adopted value of H_0 . (Only RSA galaxies with known redshifts as of that date are plotted in this figure.) A correction for internal absorption was applied to the late type spirals in the RSA sample, while none has been applied here. Hence the two samples are comparable in their luminosity range; we are in fact seeing quite far below L^* in the HDF sample.

Relative to the median galaxy in R at $z = 0.3$ the absolute magnitudes of the median galaxies with $z = 0.6, 0.8, 1.2$ are $-1.8, -2.6, -3.6$ smaller due solely to the larger distance using our

adopted cosmology.⁸ The median (in z) galaxies in the intermediate and high redshift intervals have absolute magnitudes -1.1 and -1.9 smaller than the median in the low z interval. It can be argued that about half of this luminosity selection is appropriate because it compensates passive stellar evolutionary effects. However, taking a strictly morphological approach, we have ignored this and simply make comparative observations about galaxies with similar luminosities to those at high redshift. Our prime conclusions are quite robust to this choice. However, luminosity selection is a serious concern when probing the evolution of secondary characteristics such as disk surface brightness (Simard *et al.* 1999).

2.3. Sampling

An additional and related caveat concerns the size of the sample and the sensitivity to fluctuations resulting from the luminosity selection. A good measure of this is the number density of L^* galaxies, specifically Φ^*V_c , where V_c is the comoving volume and L^* , Φ^* are determined locally, expected in our three redshift intervals (*cf* Ferguson *et al.* 2000). This corresponds to 8, 10, 20 bright galaxies on the HDF and nine times as many galaxies in the FF. However, galaxies are strongly clustered and the fluctuations over small comoving volumes are much larger than Poissonian. Furthermore, the HDF was carefully selected to avoid bright galaxies (Ferguson *et al.* 2000) and there is a clear deficit of these for $z \lesssim 0.3$ (Cohen *et al.* 2000). In particular the nature of the galaxian population in the fields studied in the present investigation might have been affected by the vagaries of the density-morphology relation (Dressler 1980) along the line of sight. This concern dictated our choice of $z = 0.25$ as the lower limit of our redshift intervals.

2.4. Morphological typing

The morphological classifications reported in this paper were made by SvdB, and are on the DDO system of van den Bergh (1960abc). The images were supplied to him as $20'' \times 20''$ thumbnails along with the redshift interval and no other information. The areal scale on the sky per pixel was the same for all the images. All images were inspected, excepting those where there were serious crowding or edge effects. The classifications for the three redshift intervals, along with commentary, are presented in Tables 1-3. The R magnitudes from Hogg *et al.* (2000), the redshifts from Cohen *et al.* (2000), and the rest frame B luminosities from Cohen (2000) are also given. See Cohen (2000) for the definition of the rest frame luminosity and how it is derived.

The fractions of galaxies by type are collected in Table 4. (Intermediate types, such as Ir/Merger, are counted as 0.5 Ir and 0.5 Merger.) In the present paper we have, following van den Bergh *et al.* (1996), used the somewhat judgemental term “protogalaxy” to denote objects that

⁸In this paper, we assume a flat universe with $\Omega_M = 0.3$, $h = 0.7$ and age $t_0 = 14$ Gyr.

resemble the prototypical galaxy H36555-1249, which is shown in Figure 7. A color image of this object, which is shown as Plate 9 of van den Bergh *et al.* (1996), shows what appears to be a reddish off-center nuclear bulge that is embedded in a rather chaotic looking disk which contains half a dozen bright blue knots. Objects with this type of morphology were regarded as spirals that are still in the process of being assembled. In objects described as “mergers” the individual components/knots have not yet combined to form a single coherent structure.

3. Galaxy morphology at high and low redshift

As explained in the introduction, we interpret distant galaxies by reference to their local counterparts, as exemplified by the Shapley-Ames galaxies (van den Bergh 1960c, Table 4). The differences are striking.

3.1. Spirals

The present sample of galaxies shows an almost complete absence of “grand design” spirals, i.e. disk systems with well-developed long arms of DDO types Sb I, Sbc I and Sc I (*cf* van den Bergh *et al.* 1996). Previous experience (van den Bergh 1989), which was confirmed by radial velocity observations (Visvanathan & van den Bergh 1992), showed that such luminous grand design spirals could have been recognized on images that contain as few as ~ 100 silver grains.

Even less pronounced spiral structure, such as is seen in nearby spirals of DDO luminosity classes II, III and IV, appears to be rare in distant HDF + FF galaxies. Furthermore the spiral structure that is observed in such distant spirals appears to be more chaotic (*i.e* less regular) than do Sc and Scd spirals at $z \sim 0$. The fraction of Sc, Sc/Ir galaxies increases from $\sim 5\%$ at $z \sim 1$ to $\sim 10\%$ at $z \sim 0.5$ and $\sim 23\%$ at $z \sim 0$. Most of the missing Sc, Scd and Sc/Ir galaxies at $z \sim 1$ are probably masquerading under the categories “Protogalaxy”, “Peculiar” or “Merger”. In intermediate and early-type “spirals” little (or no) evidence is actually seen for spiral arms. At $z \sim 0.8$ this effect might be partly (but not entirely) due to the low spatial resolution with which galaxies at such large redshifts are viewed. However, at $z \sim 0.4$ the almost complete absence of well-developed spiral arms is certainly real. This is so because the mean luminosity of the galaxies in the present sample increases with redshift. Since the strength of spiral structure increases with luminosity one would actually have expected the strength of spiral arms to increase with z . In view of the fact that little or no spiral structure is actually seen at $z \gtrsim 0.5$ the Sa, Sb and Sc classifications listed in Tables 2 and 3 are almost entirely based on central concentration of light in the galaxy images. In other words spiral arm tilt and resolution could usually not be factored in to the present classifications of the most distant early-type and intermediate-type spirals.

3.2. Barred spirals

Another striking feature of the present HDF + FF sample is the almost complete absence of barred spirals at high redshift. The highest redshift galaxy that almost certainly has a real bar is at $z = 0.321$, although two possible barred galaxies in Table 1 have redshifts $z = 0.457, 0.475$ and one from Table 3 has $z = 0.962$.⁹ Taken at face value this result suggest that only $\lesssim 1\%$ of all high redshift galaxies are barred spirals, compared to 21% to 34% among nearby spirals (van den Bergh 1998, p.43).

3.3. Ellipticals

Roughly one fifth of the galaxies with $z \sim 1$ are compact, and have morphologies similar to those of nearby E, S0 and Sa galaxies. The data in Table 4 show no statistically significant variation with redshift in the fraction of field galaxies with classification types E, E/S0 and S0.

It is interesting to note evidence from the morphological classification for at least one density enhancement along the line of sight to the HDF which contains a clump of nine E0 – E3 galaxies with $< z > = 0.679$. This is one of the most prominent peaks in the redshift distribution of galaxies in the region of the HDF, and was noticed as such in the initial redshift survey analysis of Cohen *et al.* (1996).

3.4. Peculiar-merging galaxies

Distant galaxies are far more likely to be classified as peculiar. Van den Bergh (1960c) found only 31 out of 540 (5.7%) of all nearby spirals of types Sa, Sb and Sc in the Shapley-Ames catalog to be peculiar. After excluding edge-on objects (in which it is difficult to detect any peculiarities), one finds that 17.5 out of 20.5 (85%) of all spirals with types Sa–Sab–Sb–Sbc–Sc and redshifts of $0.25 < z < 0.60$ are noted as being peculiar in Table 1. Only four out of seven objects of types Sa–Sab are peculiar, whereas all spirals of types Sb–Sbc–Sc are found to be peculiar. Perhaps surprisingly, Table 4 shows that the fraction of peculiar galaxies appears to remain approximately constant over the range $0.25 < z < 1.2$. The reason for this is, no doubt, that it is much easier to see peculiarities in the relatively large images of nearby galaxies at $z \sim 0.4$ than it is to notice similar peculiarities in the much smaller images of very distant galaxies with $z \sim 1$.

Similarly, galaxies classified as probable mergers, and which account for only $\sim 1\%$ of the galaxies at $z \sim 0$, represent $\sim 6\%$ of those with $0.25 < z < 0.80$ and for 14% at $z \sim 1$. In particular, there is a rapid increase with redshift in the fraction of triple and multiply interacting galaxies. In

⁹ Bunker *et al.* (2000) claim that this object (H36483_1214), “seems to be a chance alignment of a swath of young stars with the approximate axis of the true bar.”

fact, some small regions of the Hubble Deep Field could be described as debris fields filled with fragments that might eventually merge into one or more major galaxies.

4. Discussion

Butcher & Oemler (1978) first established that cluster galaxies evolve with time. The observations presented here (and in earlier studies cited above), firmly establish that the morphology of field galaxies also evolves over time. The challenge now is to use these empirical observations to infer a physical description of galaxy formation and evolution. (This approach is quite complementary to deductive methods that use “semi-analytic” extensions to gravitational instability theory to make quantitative comparison with measured properties of galaxies.) The most natural way to address this problem is to take the galaxies we see around us today and to ask, in a statistical fashion, what are their histories. However, this will almost certainly lead to an incomplete view because galaxies interact and merge and are otherwise strongly affected by their environment. In addition many galaxies may become too dim to be observable locally.

4.1. Spirals

The low fraction of Sc and Sc/Ir galaxies at high redshift and the almost complete absence of luminous, “grand-design” galaxies beyond $z \sim 0.3$, when the universe had an age of ~ 10 Gyr, suggests that a major fraction of the future Sc galaxies are still classified as protogalaxies or mergers at $z \sim 1$, ($t \sim 8$ Gyr). In other words many Sc galaxies had not yet fully assembled at this time. This is supported by the observation that most early-type spirals in the field already appear to have achieved a more-or-less “normal” morphology by $z \sim 0.4$, while late-type spirals still look peculiar. However, it should be emphasized that the individual bits and pieces from which Sc galaxies were assembled might contain quite old stars and clusters.

This deduction, in conjunction with the fact that significant numbers of compact early-type galaxies are observed at high redshifts, may support the view of Boissier & Prantzos (2000) that the time-scale for the formation of low-mass disks is longer than that for more massive ones. This, in turn, is consistent with the view (Bell & de Jong 2000) that it is the surface density of a young galaxy that drives its rate of star formation. As Boissier & Prantzos point out, this interpretation may present some difficulties for the standard picture of hierarchical cosmology.

The observation that spiral structure is often poorly developed in galaxies with $z > 0.5$ is perhaps not surprising. The rotational period in the outer parts of a giant galaxy ranges from $\sim 0.3 - 1$ Gyr and density wave theory requires several rotational periods for the arms to develop fully. Even if a disk forms when the universe is, say, 2 Gyr old, there may be only time for ~ 5 rotational periods before it appears in our high redshift interval. This constraint is particularly relevant to the grand design spirals, which may not assemble as disks till the universe was $\gtrsim 5$ Gyr

old and then take another ~ 5 Gyr to develop their arms. In this connection it is of interest to note (Fasano *et al.* 2000) that the galaxian population of rich clusters changed significantly even more recently, with spirals being transformed into S0 galaxies between $z \sim 0.1$ and $z \sim 0.25$. Such a transformation of spirals into S0 galaxies might have been produced by ram pressure stripping (Gunn & Gott 1972) or by galaxy harassment and tidal effects (Abadi, Moore & Bower 1999, Quillen, Moore & Bower 2000).

4.2. Barred spirals

Our observations suggests that most genuine barred spirals only started to form ~ 4 Gyr ago. This may be because galaxies at large z are still too young to have formed dynamically cool disks which permit bar-like instabilities to develop. In this connection it is of interest to note that a number of Sb galaxies at $z \sim 1$ appear to have real bulges. (Good examples are F36254_1519), F36481_1102 and F37088_1117). It would be important (but difficult) to do accurate photometry of these spirals to determine if the cores in these galaxies are true $R^{1/4}$ bulges¹⁰ or if they are just the brightest inner parts of exponential disks. If the presence of true bulges at $z \sim 1$ were to be confirmed this would militate against the hypothesis of Raha *et al.* (1991) and of Pfenniger, Martinet & Combes (1996) that some bulges might have been formed from bars.

4.3. Ellipticals

This study does not shed much light on the evolution of elliptical galaxies, which appear to have mostly formed by $z \sim 1$. The major uncertainty is whether the compact galaxies that are classified as E, S0 or Sa at $z \sim 1$ are really bulges or if we are already observing disks (*cf* Marleau & Simard 1998). This is a crucial test for theories of galaxy formation. However, this issue is complicated by the observation (Graham & Prieto 1999) that the bulges of many late-type spirals are best described by exponential luminosity profiles.

4.4. Peculiar-merging galaxies

Among nearby NGC galaxies perhaps only $\sim 0.1\%$ are members of multiple interacting-merging systems that resemble Stefan's Quintet (NGC 7317-19). On the other hand a significant fraction of the present sample of HDF and FF objects appear to be members of (or associated with) multiple merging systems. This result is consistent with the view (Toomre 1977, Abraham 1999, Carlberg *et al.* 2000, Le Févre *et al.* 2000) that mergers were much more frequent in the past than they are

¹⁰Falomo *et al.* (1997) have previously established that a compact galaxy with $z = 0.19$ has an $R^{1/4}$ profile.

at the present time. However, debate continues (*eg* Carlberg *et al.* 2000) about the rate at which such mergers increase with redshift, and regarding the mass range of merging galaxies.

An important caveat is that some close pairs may consist of projected superposed images of unrelated galaxies. In all four cases where the redshifts of both of a pair of galaxies SvdB considered to be mergers are known, the redshifts are discrepant, and the objects do not appear to be physically associated. (See the notes to Tables 1, 2 and 3.) ¹¹ This serves again as a warning that, in the absence of measured redshifts for all component galaxies, only obvious tidal distortions should move a “merger suspect” into the “merger” category.

4.5. Morphological classification at high redshift

Van den Bergh *et al.* (1996) pointed out that many of the images of very distant HDF and FF galaxies do not fit comfortably into the Hubble (1936) classification scheme which we now find to be only strictly applicable to field galaxies with $z \lesssim 0.3$. In particular, since spiral structure was rare (or absent) prior to this time, the DDO luminosity classification system (van den Bergh 1960abc, Sandage & Tammann 1981) is not especially useful.

Can we devise a galaxy classification scheme that would have been useful to sapient beings who might have been surveying galaxies in their neighborhood some 5 Gyr ago? Unfortunately the search for such a system is made more difficult by the fact that it is often not clear if adjacent luminous clumps should be regarded as separate galaxies, or as condensations within a single larger protogalaxy. In fact such a dichotomy is not even physically significant if initially separate ancestral bits and pieces eventually merge into a single galaxy. Possibly a two-parameter classification system based on central concentration of light (Morgan 1958, 1959) and asymmetry (Abraham *et al.* 1996b) or clumpiness, perhaps supplemented by color information, may represent the best that can be done regarding the classification of galaxies in the early universe. In rich nearby clusters only the central concentration of light appears to be a useful classification parameter.

In this study we have used redshift data and the FF images to substantiate many of the original reactions to the first inspection of the HDF over four years ago. In addition we have shown that the development of spiral structure, both wound and barred, is delayed until the universe is typically ~ 10 Gyr old. Perhaps the most pressing current task is to determine if the compact objects observed at $z \sim 1$ are disks or spheroids. Overall, though, we remain impressed by the strong evolution in galaxy morphology. As Hartley (1953) wrote in *The Go-between* “The past is a foreign country; they do things differently there.”

¹¹In one of the four cases, one of the redshifts is uncertain. In the other three cases, Cohen *et al.* (2000) regard both redshifts as secure.

It is a pleasure to thank Peter Stetson for his help with the re-scaling of the present images, Simon Morris for cosmological consultations, and Jerry Sellwood for information on the formation of galactic bars. The extragalactic work of JGC, who is the PI of the Caltech Faint Galaxy Redshift Survey, is not supported by any Federal agency. RB acknowledges support under NSF grant AST-9900866.

REFERENCES

Abadi, M. G., Moore, B. & Bower, R. G., 1999, MNRAS, 308, 947

Abraham, R. G. 1999, in *Interactions of Galaxies at Low and High Redshifts*, Eds. J. E. Barnes and D. B. Sanders (Dordrecht:Kluwer), p.11

Abraham, R. G., 2000, *Toward a New Millennium in Galaxy Morphology*, eds. D. L. Block *et al.* (Dordrecht: Kluwer) in press, (astro-ph/0006166)

Abraham, R. G., Tanvir, N. R., Santiago, B. X., Ellis, R. S., Glazebrook, K. & van den Bergh, S., 1996b, MNRAS, 279, L47

Abraham, R. G., Ellis, R. S., Fabian, A. C., Tanvir, N. & Glazebrook, K. 1999a MNRAS, 303, 641

Abraham, R. G., Merrifield, M. R., Ellis, R. S., Tanvir, N., Brinchmann, J. 1999b, MNRAS, 308, 569

Abraham, R. G., van den Bergh, S., Glazebrook, K., Ellis, R. S., Santiago, B.X., Surma, P. & Griffiths, R.E., 1996b, ApJS, 107, 1

Ames, M., 1997, The (London) Times, 1997 August 21

Bell, E. F. & de Jong R. S., 2000, MNRAS, in press

Boissier, S. & Prantzos, N., 2000, MNRAS, 312, 398

Brinchmann, J. *et al.* 1998, ApJ, 499, 112

Bunker, A., Spinrad, H., Stern, D., Thompson, R., Moustaka, L., Davis, M. & Dey, A., 2000, to appear in *Galaxies in the Young Universe*, ed. H. Hippelein & K. Meisenheimer, astro-ph/0004348

Butcher, H. & Oemler, G., 1978, ApJ, 219,18

Carlberg, R. G . *et al.* 2000, ApJ, 532, L1

Cohen, J. G., 2000, AJ (submitted)

Cohen, J.G., Cowie, L.L., Hogg, D.W., Songaila, A., Blandford, R., Hu, E.M. & Shopbell, P., 1996, ApJ, 471, L5

Cohen, J. G., Hogg, D. W., Blandford, R. D., Cowie, L. L., Hu, E., Songaila, A., Shopbell, P. & Richberg, K., 2000, ApJ, 538, 29

Corbin, M. R., Vacca, W. D., O'Neil, E., Thompson, R. I., Rieke, M. J., & Schneider, G., 2000, AJ, 119, 1062

Cowie, L. L., Hu, E. M. & Songaila, A., 1995, AJ, 110, 1576

Dressler, A., 1980, ApJ, 236, 351

Driver, S. P., Fernandez-Soto, A., Couch, W. J., Odewahn, S. C., Windhorst, R. A., Phillipps, S., Lanzetta, K., & Yahil, A., 1998, ApJ, 496,L93

Eskridge, P. B. *et al.* 2000, AJ, 119, 536

Falomo, R., Urry, C. M., Pesce, J. E., Scapa, R., Giavalisco, M. & Treves, A., 1997, ApJ, 476, 113

Fasano, G., Poggianti, B. M., Couch, W. J., Bettoni, D., Kjaergaard, P. & Moles, M., 2000, ApJ (in press) (astro-ph/0005171)

Ferguson, H. C., Dickinson, M. & Williams, R., 2000, ARAA (in press)

Graham, A. W. & Prieto, M., 1999, ApJ, 524, L23

Gunn, J. E. & Gott, J. R., 1972, ApJ, 176, 1

Hartley, L. P., 1953 *The Go-Between*, (London: H.Hamilton)

Hogg D. W., Pahre M. A., Adelberger K. L., Blandford R., Cohen J. G., Gautier T. N., Jarrett T., Neugebauer G. & Steidel C. C., 1999, ApJS, 127, 1

Hubble, E. 1936, *The Realm of the Nebulae*, (New Haven: Yale University Press), p.45

Le Févre, O. *et al.* 2000, MNRAS, 311, 565

Lilly, S. *et al.* 1998, ApJ, 500, 75

Marleau, F. R. & Simard, L., 1998, ApJ, 507, 585

Morgan, W. W., 1958, PASP, 70, 364

Morgan, W. W., 1959, PASP, 71, 394

Odewahn, S. C., Windhorst, R. A., Driver, S. P. & Keel, W. C., 1996, ApJ, 472, L13

Pfenniger, D., Martinet, L. & Combes, F., 1996, in *New Extragalactic Perspectives in South Africa*, ed. D.L.Block & J.M.Greenberg, (Dordrecht: Kluwer), p.291

Quilis, V., Moore, B. & Bower, R., 2000, Science, 288, 1617

Raha, N., Sellwood, J.A., James, R.A. & Kahn, F.D., 1991, Nature, 352, 411

Sandage, A. & Tammann, G. A., 1981, *A Revised Shapley-Ames Catalog of Bright Galaxies*, (Washington: Carnegie Institution)

Schade, D., Lilly, S.J., Crampton, D., Ellis, R.S., Le Févre, O., Hammer, F., Brinchmann, J., Abraham, R., Colless, M., Glazebrook, K., Tresse, L. & Broadhurst, T., 1999, ApJ, 525, 31

Simard, L., Koo, D.C., Faber, S.M., Sarjedini, V.L., Vogt, N.P., Phillips, A.C., Gebhardt, K., Illingworth, G.D. & Wu, K.L., 1999, ApJ, 519, 563

Toomre, A., 1977, in *The Evolution of Stellar Populations*, Eds. B. M. Tinsley & R. B. Larson, 1977 (New Haven: Yale Observatory), p.420

van den Bergh, S., 1960a, ApJ, 131, 215

van den Bergh, S., 1960b, ApJ, 131, 558

van den Bergh, S., 1960c, Pub.David Dunlap Obs., 2, 159

van den Bergh, S., 1989, AJ, 97, 1556

van den Bergh, S., 1998, *Galaxy Morphology and Classification*, (Cambridge: Cambridge Univ. Press)

van den Bergh, S., Abraham, R. G., Ellis, R. S., Tanvir, N. R., Santiago, B. X. & Glazebrook, K. G., 1996, AJ, 112, 359

van den Bergh, S. & Pierce, M. J. 1990, ApJ, 364, 444

Visvanathan, N. & van den Bergh, S., 1992, AJ, 103, 1057

Williams, R. E. *et al.* 1996, AJ, 112, 1335

Table 1. Red Images of Galaxies with $0.25 < z < 0.60$

ID ^a	Redshift ^b	R^c (Mag)	Log[$L(B)$] ^d (W)	Classification	Comments
F36427_1306	0.485	22.02	36.10	Sab/S0 (edge-on)	Projected on merger remnant
F36446_1304	0.485	21.14	36.57	Sb pec + Ir/Pec	Knots, but no arms,in disk ^e
F36454_1325	0.441	22.33	36.31	Pec	High SB
F36458_1325	0.321	20.71	36.23	Sc pec	Only rudimentary spiral structure in disk
F36563_1209	0.321	23.22	35.34	Sb pec	Knots,but on arms,in disk
F36575_1212	0.561	22.62	36.17	Ir/Merger	
H36413_1141	0.585	21.91	36.32	Sab	Merging with H36414_1142 ^f
H36414_1142	0.548	23.51	35.92	Merger	At least three components ^f
H36416_1200	0.483	25.03	35.16	S/Ir	
H36419_1205	0.432	20.82	36.63	Sb pec	Faint outer arms surrounding bright core with incipient arms
H36429_1216	0.454	20.51	36.79	Sc pec	High SB. Two chaotic arms
H36439_1250	0.557	20.84	36.89	Sc pec	Knot plus incipient arm in disk
H36442_1247	0.555	21.40	36.64	S pec	Proto-bulge but no arms (yet?)
H36448_1200	0.457	22.85	35.89	S(B?)cd:	
H36465_1203	0.454	24.32	35.44	Sa pec	Asymmetric + tidal debris
H36465_1151	0.503	22.00	36.42	E1	
H36470_1236	0.321	20.62	36.42	S pec	E3-like core embedded in chaotic spiral(?) envelope
H36472_1230	0.421	22.63	35.91	Sab pec	
H36480_1309	0.476	20.43	36.92	Sa:	
H36489_1245	0.512	23.48	35.76	E:5 pec	Asymmetric core embedded in fuzz
H36493_1311	0.477	21.97	36.30	E1	
H36494_1316	0.271	23.63	35.16	Pec	
H36496_1257	0.475	21.91	36.31	Sa pec	Asymmetric, multiple nuclei
H36497_1313	0.475	21.46	36.38	Sb pec	Asymmetric
H36501_1239	0.474	20.43	36.87	Pec	Has high SB central region
H36508_1251	0.485	23.15	35.89	?	Disk containing multiple knots
H36508_1255	0.321	22.27	35.83	S pec	Nucleus plus two knots in disk
H36513_1420	0.439	23.22	35.74	Sb pec	Disk with no spiral arms. Off-center nucleus
H36516_1220	0.401	21.45	36.32	Sab pec	
H36517_1353	0.557	21.08	36.80	Sb pec/Merger	Double nucleus

Table 1—Continued

ID ^a	Redshift ^b	<i>R</i> ^c (Mag)	Log[L(<i>B</i>)] ^d (W)	Classification	Comments
H36519_1209	0.458	22.75	35.94	Pec	E1-like bulge embedded in asymmetric envelope
H36519_1400	0.559	23.03	36.00	Sb pec (edge-on)	Off-center core
H36526_1219	0.401	23.11	35.72	E:4	
H36528_1404	0.498	23.45	35.82	Pec/Merger	
H36534_1234	0.560	22.78	36.11	Sb pec	Off-center bulge
H36536_1417	0.517	23.36	35.82	Sb pec (edge-on)	Nucleus + two knots in disk
H36549_1314	0.511	23.81	35.68	Pec (edge-on)	Disk with nucleus + two knots
H36551_1311	0.321	23.58	35.33	Pec	
H36554_1402	0.564	23.08	35.96	Sbc pec	Off-center nucleus + one knot in disk
H36555_1359	0.559	23.74	35.73	Sb (edge-on)	
H36560_1329	0.271	23.80	35.16	Ir/Pec	
H36566_1245	0.518	20.06	37.11	Sb pec	Bright E2-like bulge without spiral arms. See Fig. 8
H36569_1258	0.520	23.84	35.76	Sa	
H36571_1225	0.561	22.36	36.27	Sc pec	Has one incipient spiral arm + three knots. See Fig. 9
H36572_1259	0.475	21.07	36.61	SB? pec	Bar or two knots
H36580_1300	0.320	22.04	35.89	Merger	Two nuclei
H36587_1252	0.321	20.99	36.27	SBbc pec	Probable bar in asymmetric two-armed spiral. See Fig. 10
H36594_1221	0.472	23.53	35.67	S? + Ir: ^g	
H37005_1234	0.563	21.43	36.74	S0/Star	

^aNames are Habcde_fghi for objects in the HDF, where the object's J2000 coordinates are 12 ab cd.e +62 fg hi. The initial letter is "F" for objects in the flanking fields.

^bRedshifts are from Cohen *et al.* (2000).

^c*R* magnitudes are from Hogg *et al.* (2000).

^dRest frame *B* luminosities are from Cohen (2000). $M_B = -21.0$ (rest frame) $\equiv \log[L(B)]$ (W) = 36.9.

^eThe Sb pec is the object for which a redshift exists. The redshift of the fainter second galaxy is unknown.

^fThe redshifts of this pair are not consistent with a merger, but the redshift of H36414_1142 is uncertain.

^gThis is a close pair of faint galaxies separated by about 1 arcsec. It is not clear which of them (or perhaps both of them) was included in the spectroscopic observations.

Table 2. Infrared Images of Galaxies with $0.60 < z < 0.80$

ID ^a	Redshift ^b	<i>R</i> ^c (Mag)	Log[<i>L</i> (<i>B</i>)] ^d (W)	Classification	Comments
F36194_1428	0.798	22.60	36.61	Ir?	Multiple nuclei
F36244_1454	0.628	20.34	37.34	E2	
F36243_1525	0.682	22.78	36.48	E:3 pec	Asymmetrical
F36247_1510	0.641	20.41	37.26	Sa	
F36249_1252	0.631	22.76	36.22	Ir (edge-on)	
F36250_1341	0.654	24.32	35.73	Star/E0	
F36254_1519	0.642	21.82	36.60	Sb pec	Slightly asymmetrical
F36270_1509	0.794	21.60	37.36	Sa	
F36275_1418	0.751	22.37	36.54	S (edge-on)	
F36284_1037	0.760	22.76	36.39	E0	
F36287_1357	0.639	23.05	36.10	Sb pec?	
F36290_1346	0.693	23.02	36.25	E:2	Compact
F36297_1324	0.758	23.25	36.23	Pec/Merger?	Member of a compact group
F36297_1329	0.748	23.03	36.44	Pec	Member of a compact group
F36299_1403	0.793	21.97	36.91	Merger?	
F36334_1432	0.748	23.08	36.31	S: pec	In compact group
F36340_1054	0.762	21.55	36.87	Ir or protogalaxy	In a group
F36362_1319	0.680	22.20	36.44	Lumpy protogalaxy?	
F36370_1159	0.779	21.56	36.84	Proto Sc?	
F36379_0922	0.767	21.43	37.08	Sb: pec	Has two “nuclei”, not a bar!
F36384_1312	0.635	22.27	36.38	Sb pec	
F36390_1006	0.635	21.22	36.81	?	Has double core
F36405_1003	0.749	22.39	36.58	Sc:	
F36415_0902	0.713	22.31	36.59	?	
F36427_1503	0.698	23.17	36.18	Pec	
F36454_1523	0.683	22.06	36.57	S:	
F36481_1102	0.650	22.58	36.40	Sb	
F36481_1002	0.682	21.92	36.60	Ir/Pec	
F36499_1058	0.684	22.63	36.36	Sa:	
F36575_1210	0.665	21.10	36.98	E:0 + Sb:	2nd gal. is F36575_1211 ^e
F36580_1137	0.681	23.00	36.17	E:1	
F36588_1434	0.678	20.85	37.14	S pec	
F36598_1449	0.762	21.62	37.04	S + Sb	Merger
F37015_1129	0.779	21.45	37.07	Merger	Has three nuclei. In group

Table 2—Continued

ID ^a	Redshift ^b	<i>R</i> ^c (Mag)	Log[<i>L</i> (<i>B</i>)] ^d (W)	Classification	Comments
F37017_1144	0.744	22.10	36.71	Sa:	Multiple nuclei?
F37020_1517	0.744	23.56	36.24	Sab:	
F37036_1353	0.745	21.63	36.78	Sb pec	
F37058_1317	0.753	21.95	36.74	Sc:	
F37061_1332	0.753	21.85	36.83	Sbc pec	Multiple nuclei?
F37069_1208	0.693	24.13	35.78	E:0	
F37072_1214	0.655	22.19	36.62	Sb	
F37074_1356	0.752	23.65	36.19	Sa	
F37080_1246	0.654	21.80	36.64	Sb	
F37083_1320	0.785	22.86	36.44	Pec	Tadpole-like
F37088_1117	0.639	23.05	36.18	Sb pec	Asymmetrical
F37088_1214	0.788	23.90	36.05	Sa	
F37105_1141	0.789	21.20	37.10	Sb pec + S	
F37107_1431	0.677	22.39	36.61	E1	
F37108_1059	0.747	24.25	36.05	? + ?	Low SB
F37113_1545	0.692	22.43	36.42	dIr?	Low SB
F37115_1042	0.778	21.97	36.74	Sbc pec	
F37163_1432	0.635	22.50	36.30	Sb pec	Asymmetrical
F37192_1143	0.784	22.81	36.47	Sb pec	
F37213_1120	0.656	22.22	36.47	Sc pec	
H36389_1219	0.609	22.14	36.43	Pec	High SB. Complex core = merger?
H36436_1218	0.752	22.56	36.46	E1	
H36438_1142	0.765	21.26	37.32	E1	In group
H36459_1201	0.679	23.88	35.85	Pec	High SB. Has two cores
H36470_1213	0.677	24.63	35.51	Pec	Core + asymmetrical fuzz
H36471_1414	0.609	23.92	35.82	E5	
H36487_1318	0.753	22.87	36.40	Sc pec	Very lumpy structure. In cluster
H36494_1406	0.752	21.95	36.83	E3	
H36498_1242	0.751	24.38	35.64	dIr (edge-on)	In cluster
H36502_1245	0.680	21.74	36.86	E3	In cluster
H36538_1254	0.642	20.95	37.01	S pec	High SB
H36555_1245	0.790	23.08	36.79	S	
H36586_1221	0.682	23.40	36.03	E2	
F37222_1124	0.786	22.33	36.71	Sa	

Table 2—Continued

ID ^a	Redshift ^b	<i>R</i> ^c (Mag)	Log[<i>L</i> (<i>B</i>)] ^d (W)	Classification	Comments

^aNames are Habcde_fghi for objects in the HDF, where the object’s J2000 coordinates are 12 ab cd.e +62 fg hi. The initial letter is “F” for objects in the flanking fields.

^bRedshifts are from Cohen *et al.* (2000).

^c*R* magnitudes are from Hogg *et al.* (2000).

^dRest frame *B* luminosities are from Cohen (2000). $M_B = -21.0$ (rest frame) $\equiv \log[L(B)] = 36.9$.

^eThe redshifts of the two galaxies are both known and not consistent with a merger.

Table 3. Infrared Images of Galaxies with $0.80 < z < 1.20$

ID ^a	Redshift ^b	<i>R</i> ^c (Mag)	Log[<i>L</i> (<i>B</i>)] ^d (W)	Classification	Comments
F36175_1402	0.818	21.73	36.93	Merger	
F36176_1408	0.848	22.55	36.71	?	
F36271_1001	0.842	21.53	36.90	S pec/Merger?	
F36285_0951	1.016	23.07	36.65	Sc	
F36287_1023	0.936	22.11	36.91	Merger/Protogalaxy	Prototype. See Fig.1
F36287_1239	0.880	22.11	36.91	?	Image too small to classify
F36296_1420	1.055	24.00	36.06	Star	
F36313_1113	1.013	22.09	37.07	Ir/Merger?	Has double nucleus and a close companion
F36332_1235	1.140	23.11	36.66	Ir/Merger?	
F36336_1005	1.015	22.15	37.12	Ir/Merger	Prototype. See Fig.2
F36335_1319	0.845	21.78	37.08	Sc:	High SB spiral with lumpy disk
F36340_1045	1.011	23.25	36.56	?	Has nucleus and high SB, and possibly a tail
F36341_1305	0.847	24.24	36.13	Sb + ?	Has tidal companion of low SB
F36343_1312	0.845	23.15	36.52	S/Ir?	
F36364_1237	0.961	22.94	36.81	S	Spiral with small bulge embedded in lumpy ring
F36367_1347	0.960	20.32	37.53	Star ^e	
F36367_1213	0.846	20.86	37.44	S IV:	Looks like nearby low-luminosity spiral
F36369_1346	0.846	21.20	37.14	Sb pec	Has two nuclei. May be a merger with tidal arms
F36377_1149	0.838	22.72	36.62	Ir (edge-on)	Has clumpy structure and no nucleus
F36381_1116	1.018	22.20	36.95	Late-type	Spectrum is that of the combined light of all three components
				Ir	
				Ir	
F36382_1150	0.842	22.74	36.75	Ir	High SB irregular
F36388_1118	0.934	22.53	36.62	Merger	Has three components + possible tidal arm
F36388_1257	1.127	22.28	37.22	Ir	Has high SB
F36399_1250	0.848	22.59	37.02	Proto-spiral?	High SB object with nucleus and fuzzy tail?

Table 3—Continued

ID ^a	Redshift ^b	<i>R</i> ^c (Mag)	Log[<i>L</i> (<i>B</i>)] ^d (W)	Classification	Comments
F36399_1029	0.935	22.59	37.02	?	Nucleated object with possible tidal tail
F36408_1054	0.875	22.61	36.69	?	Compact,almost stellar
F36411_1314	1.017	23.08	36.74	E1/Sa	Nucleated objecte embedded in asymmetric fuzz
F36417_0943	0.845	22.51	37.00	Sab	
F36420_1321	0.846	23.95	36.15	Sa:	Very compact
F36425_1121	0.845	23.03	36.46	Sa pec	Asymmetric
F36435_1532	0.847	22.82	36.60	Sa pec?	
F36447_1455	0.845	22.97	36.50	?	CCD bleeding from bright nucleus?
F36459_1101	0.936	22.77	37.09	E + S	Interacting pair. Spectrum probably of combined light
F36462_1527	0.851	22.11	36.94	Ir?	Might also be galaxy disrupted by encounter with nearby E(?)
F36468_1540	0.912	22.23	36.99	Merger?	Possible double core suggests this may be merger remnant
F36469_0906	0.905	23.84	36.38	Sa:	
F36472_1628	0.873	21.69	37.46	E2	
F36477_1045	1.187	23.43	37.14	Sa t?	
F36482_1507	0.890	22.38	37.20	E4:	
F36486_1141	0.962	22.21	37.47	Sb t	Has close compact companion
F36502_1127	0.954	22.88	36.62	dIr?	Companion to F36518_1125 ^f
F36518_1125	0.919	21.62	37.13	dIr	
F36522_1537	0.936	22.74	37.26	E0/Star	
F36524_0919	0.954	22.81	37.31	E3	
F36529_1508	0.942	22.84	37.15	E0	
F36532_1116	0.942	22.08	37.15	Merger?	Complex internal structure. Has close compnions
F36539_1606	0.851	22.84	36.57	Pec	Near edge of image
F36541_1514	0.849	22.84	36.51	Pec/Ir	
F36548_1557	1.132	22.51	37.41	Sab (edge-on)	
F36577_1454	0.849	22.49	36.96	Sa	Near edge of image
F36583_1214	1.020	23.79	36.40	Sa pec	Slightly asymmetric
F36589_1208	0.853	22.32	37.00	Sb pec	One-armed spiral with

Table 3—Continued

ID ^a	Redshift ^b	<i>R</i> ^c (Mag)	Log[<i>L</i> (<i>B</i>)] ^d (W)	Classification	Comments
F36595_1153	1.021	22.54	36.88	Sb: t?	off-center nucleus Two companions included in spectrum
F37003_1616	0.913	22.33	36.94	Merger?	Edge-on Ir or merger of three components
F37007_1106	0.801	22.94	36.41	Pec	Contains one “hot” pixel
F37016_1225	0.973	23.95	36.15	Ir/Merger?	
F37016_1146	0.884	25.30	35.90	Amorphous	Might be high SB Ir
F37026_1216	1.073	24.04	36.65	S pec	Asymmetrical
F37029_1427	0.898	23.67	36.35	E1/Star	
F37041_1239	0.861	23.16	36.43	Merger?	Probably a protogalaxy or a collision remnant
F37046_1415	1.050	23.97	36.37	Sb:	
F37055_1129	1.001	22.37	36.94	Merger?	May contain second nucleus within envelope
F37058_1153	0.904	21.22	37.39	Sc	Prototype. See Fig.3. Two armed spiral
F37058_1423	0.970	22.48	37.10	?	Strongly nucleated
F37065_1512	0.840	22.94	36.48	E0/Star	Redshift refers to combined light of a and b
				S/Ir	
F37078_1605	0.936	21.88	37.27	Sc	Clumps in disk/arms
F37083_1252	0.838	22.20	36.85	Sb	
F37083_1514	0.839	21.62	37.10	Sb pec	Asymmetrical bar?
F37086_1128	0.907	22.23	36.76	Merger	At least two components, one of these is distorted
				Sc	Single nucleus embedded in clumpy envelope
F37089_1202	0.855	22.90	36.52		
F37096_1055	0.858	23.16	36.40	Ir	Ir or high SB merger
F37114_1055	0.855	22.44	36.73	S pec	Asymmetrical
F37126_1546	0.937	22.08	37.07	E1	
F37129_1028	0.858	22.62	36.73	Ir/Merger	Edge-on Ir, or two component merger
F37133_1054	0.936	21.87	36.99	Sa t?	
F37141_1044	0.821	22.32	36.70	E1	

Table 3—Continued

ID ^a	Redshift ^b	<i>R</i> ^c (Mag)	Log[<i>L</i> (<i>B</i>)] ^d (W)	Classification	Comments
F37143_1221	1.084	24.12	36.66	Sa	
F37154_1212	1.014	23.25	37.06	?	Compact, asymmetrical
F37159_1213	1.020	23.27	36.86	Sb:	Core embedded in extended (tidal?) envelope
F37167_1042	0.821	21.59	36.97	Merger	Merger prototype, see Fig. 4. Three or four components
F37180_1248	0.912	22.89	36.78	Sb:	
F37196_1256	0.909	23.31	36.67	Sa/E4	
F37221_1210	0.928	23.97	36.60	Merger	Prototypical merger. See Fig. 5. At least four components
F37224_1216	0.963	22.23	37.09	S t	One of the components of F37221_1210 ^g
H36384_1231	0.944	22.87	36.87	S	Edge-on
H36386_1233	0.904	24.04	36.18	Sab	Edge-on
H36396_1230	0.943	24.40	35.79	S + E2:	Merger
H36400_1207	1.015	22.75	37.17	Star	
H36408_1203	1.010	23.49	36.50	Pec/Ir	Distorted edge-on irregular?
H36408_1205	0.882	22.94	36.63	Star + Galaxy	
H36431_1242	0.849	22.34	37.11	E2	
H36432_1148	1.010	23.10	37.01	Sb	High SB two-armed spiral
H36441_1240	0.875	23.39	36.36	Merger	
H36443_1133	1.050	21.96	37.76	E1	
H36444_1142	1.020	24.30	36.68	Merger	Prototype. See Fig. 6. Edge-on.
H36461_1246	0.900	22.86	36.92	E1	
H36461_1142	1.013	21.52	37.39	Sab pec	
H36463_1404	0.962	21.69	37.41	Sa pec	
H36467_1144	1.060	24.23	36.55	Pec	
H36477_1232	0.960	23.80	36.48	E3	
H36483_1214	0.962	23.87	36.75	S(B)bc t	Barred, or tidally distorted, spiral
H36486_1328	0.958	23.14	36.68	Merger	Has 3 or 4 components
H36490_1221	0.953	22.59	36.81	Merger?	High SB image has core and 4 outer lumps
H36492_1148	0.961	23.26	36.69	E4/Sa	
H36493_1155	0.961	23.36	36.40	Star/E0	

Table 3—Continued

ID ^a	Redshift ^b	<i>R</i> ^c (Mag)	Log[<i>L</i> (<i>B</i>)] ^d (W)	Classification	Comments
H36503_1418	0.819	23.41	36.38	S pec	Nuclear bulge embedded in eccentric ring
H36504_1315	0.851	23.41	36.38	S pec	Has distorted disk
H36519_1332	1.087	23.59	36.76	E1/Star	
H36540_1354	0.851	22.72	36.70	S/E3 pec	Has distorted core
H36551_1303	0.952	24.29	36.51	E3	High SB
H36553_1311	0.968	22.86	37.11	E/Sa:	High SB
H36555_1353	1.147	22.85	36.90	Sc/Ir:	
H36555_1249	0.950	23.53	36.48	Protospiral	See Fig.7
H36566_1220	0.930	23.15	36.87	Sa	High SB. Has companion
H36576_1315	0.952	22.94	36.62	S/Ir	

^aNames are Habcd.e_fghi for objects in the HDF, where the object's J2000 coordinates are 12 ab cd.e +62 fg hi. The initial letter is "F" for objects in the flanking fields.

^bRedshifts are from Cohen *et al.* (2000).

^c*R* magnitudes are from Hogg *et al.* (2000).

^dRest frame *B* luminosities are from Cohen (2000). $M_B = -21.0$ (rest frame) $\equiv \log[L(B)] = 36.9$.

^eThis object is a QSO from Keck spectroscopy.

^fThese two objects have rather discrepant well determined redshifts and are probably not physically associated.

^gThese two objects have rather discrepant well determined redshifts and are probably not physically associated.

Table 4. Morphological Types of Nearby and Distant Clusters^a

Galaxy Type	Shapley-Ames $z \sim 0$ (%)	HDF 0.25 – 0.60 (%)	+	Flanking Fields 0.80– 1.20 (%)
E + S0 + E/S0	22	11	21	16
E0/Sa +S0/Sa	1	0	0	2
Sa + Sab	7	15	11	13
Sb +Sbc	27	26	23	10
Sc + Sc/Ir + Scd	23	10	5	5
Ir	2	5	7	12
S	10	11	10	11
?, Pec, Protogalaxy	7	16	19	12
Merger	1 ^b	7	4	15
Total in sample	936	50	70	120 ^c

^aDue to rounding errors percentages do not all add to 100.

^bFrom appendix to van den Bergh (1960c)

^cIncludes four extragalactic objects classified as “star” and one classified as “amorphous”

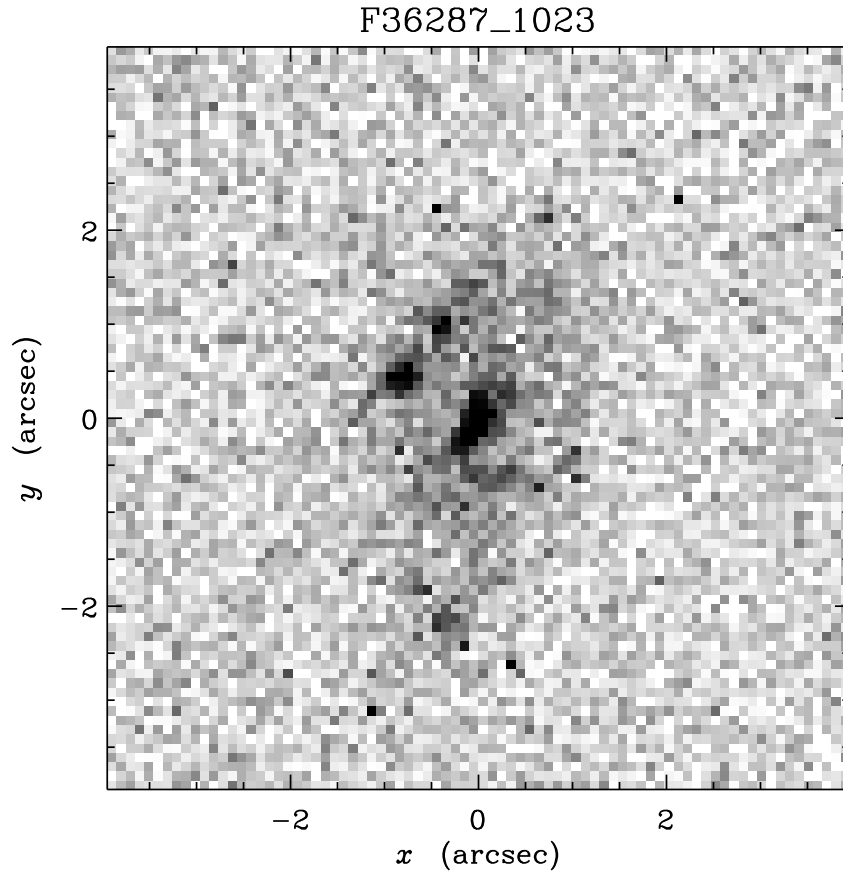


Fig. 1.— Example at $z = 0.936$ of merger of relatively low surface brightness galaxies that may eventually evolve into an Sc galaxy. In this figure, as in all the others, a 8×8 arcsec 2 section of the WFPC2/HST image is displayed in the orientation of the original HST image, whose scale is 0.1 arcsec/pixel.

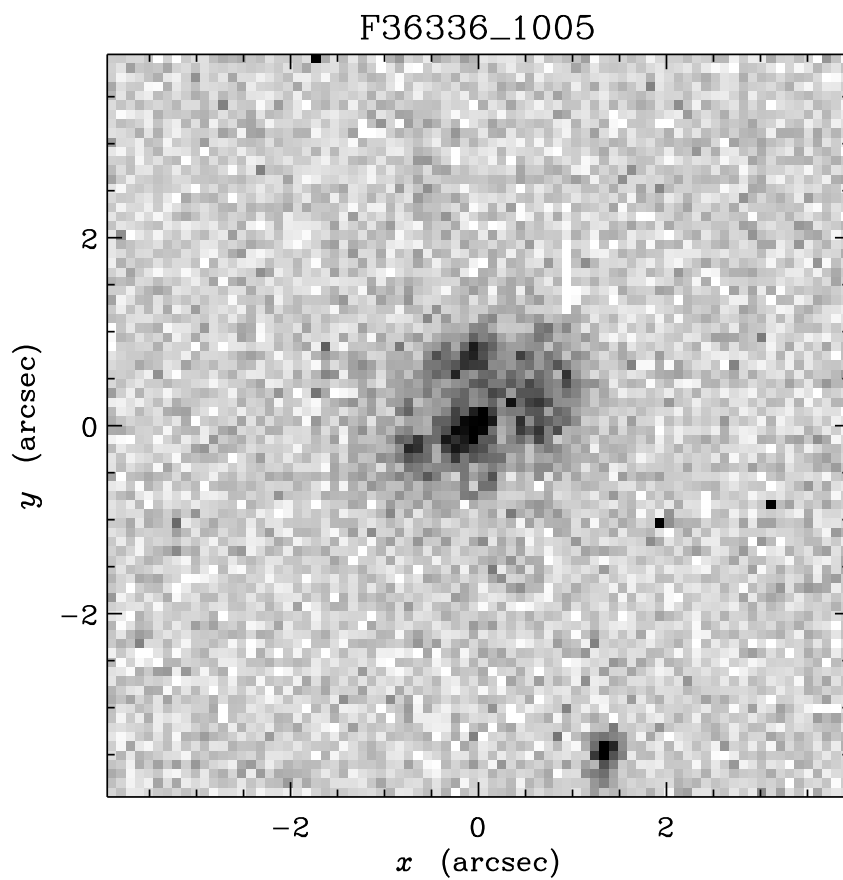


Fig. 2.— This $z = 1.015$ object might either be a distant Ir galaxy or a multi-component merger.

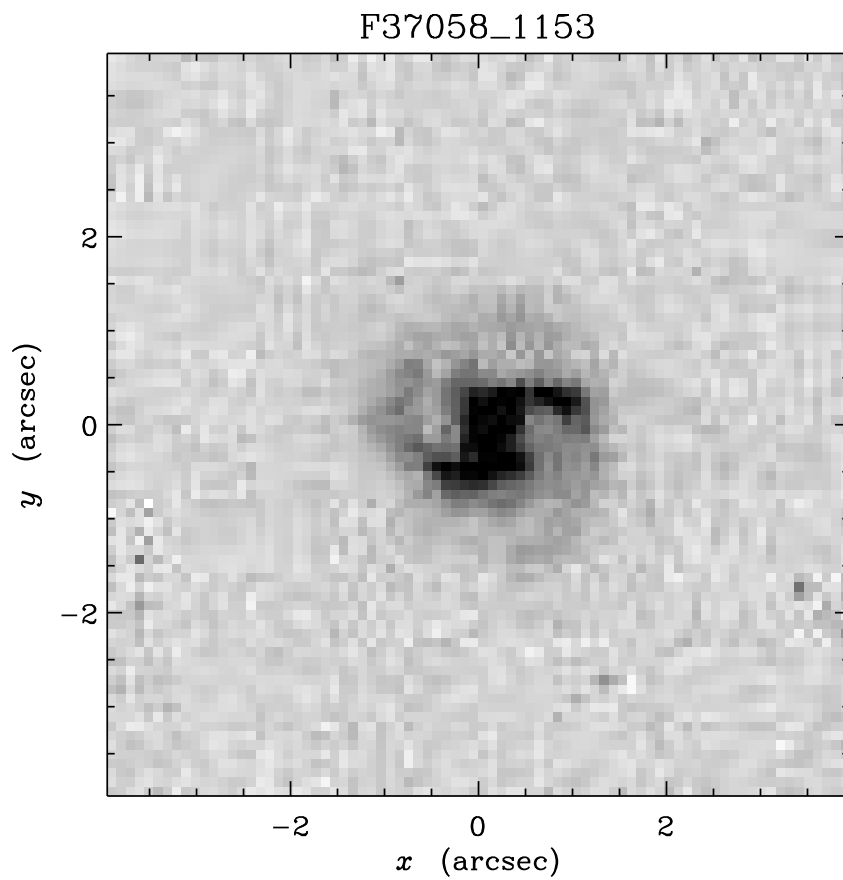


Fig. 3.— Rare example of a two-armed spiral viewed at a large look-back time ($z = 0.904$).

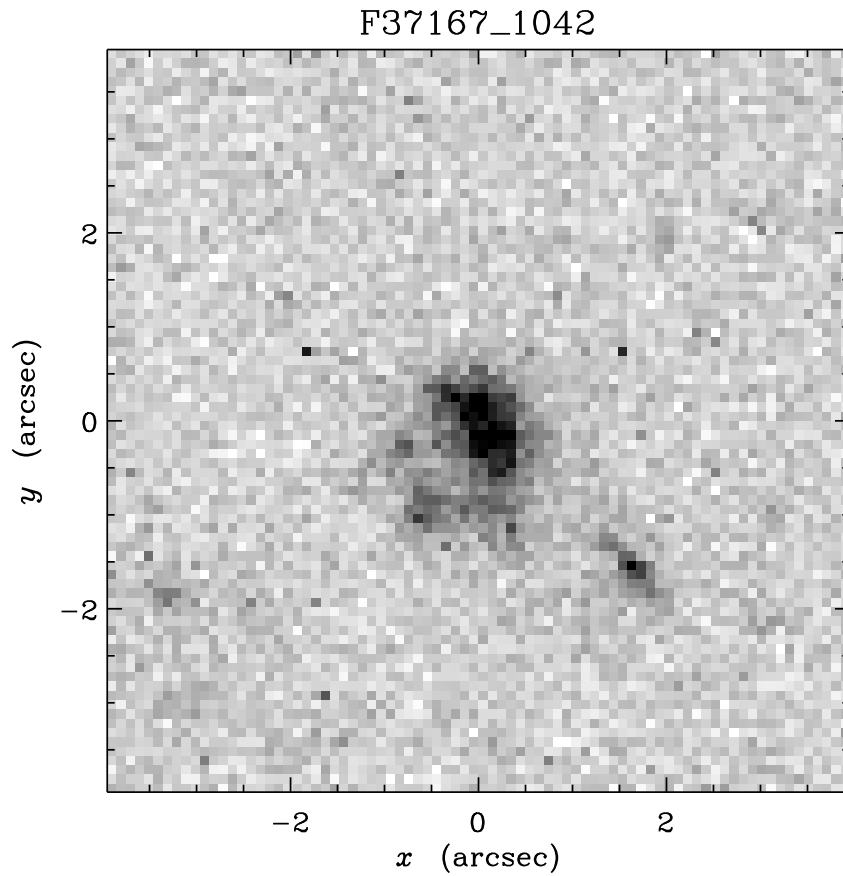


Fig. 4.— Example (at $z = 0.821$) of a possible multi-component merger. Note “bits and pieces” of other, probably more distant, objects in this field.

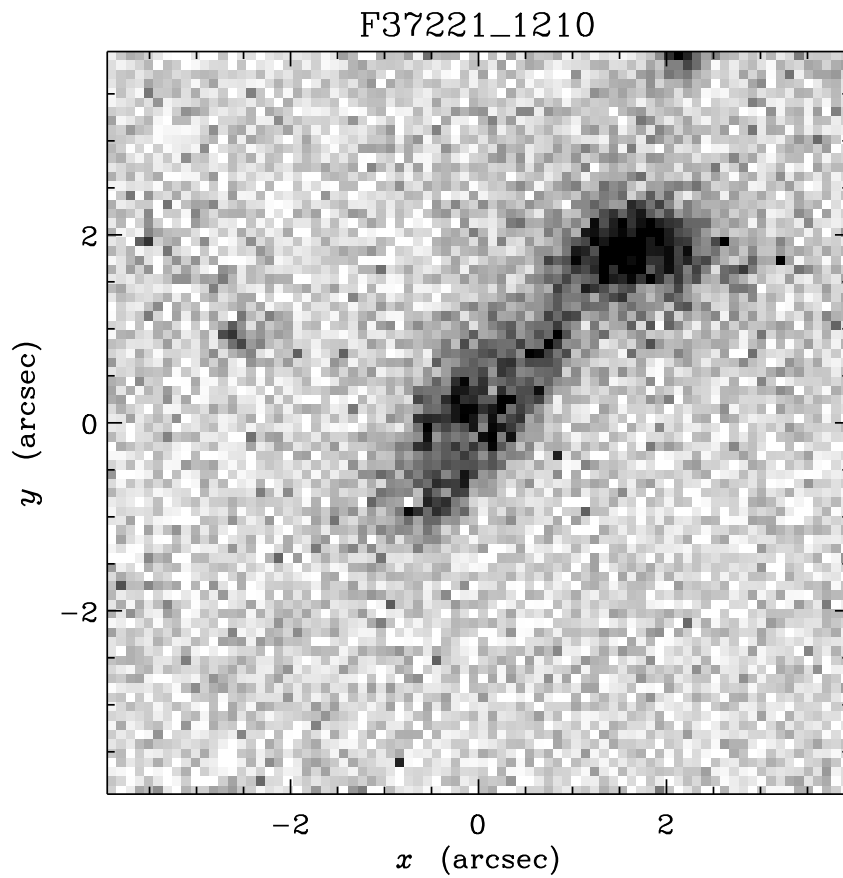


Fig. 5.— The central part of a “debris field” (with $z = 0.928$) that may eventually merge into one or more larger galaxies is shown.

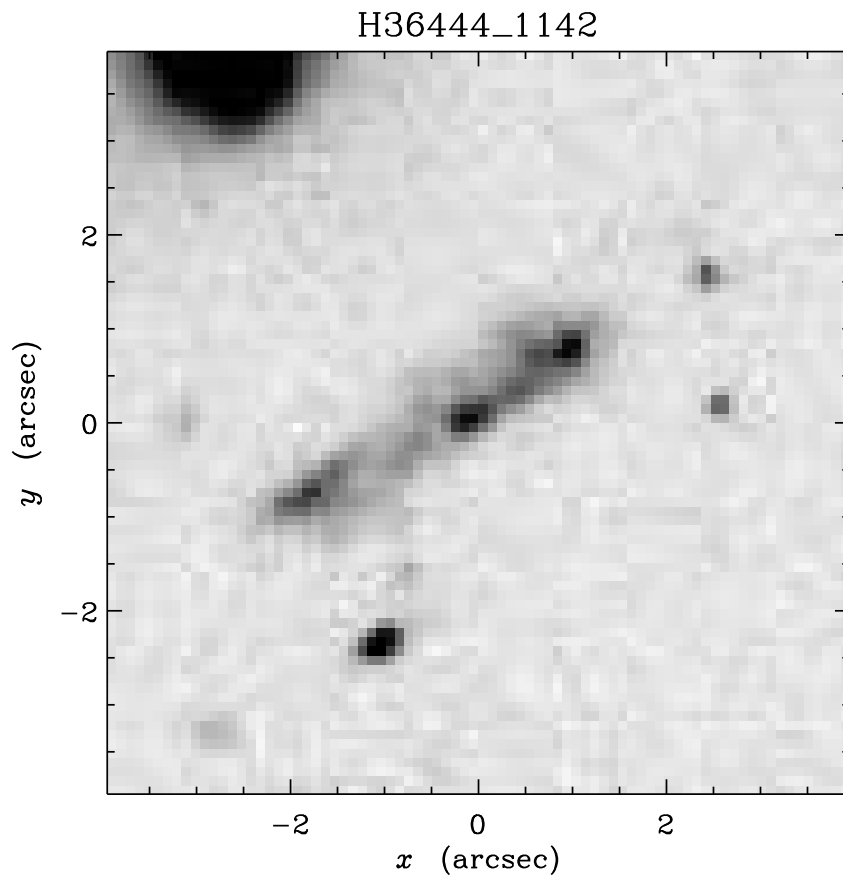


Fig. 6.— Peculiar edge-on disk or bar-like object at $z = 1.020$ containing at least three merging components.

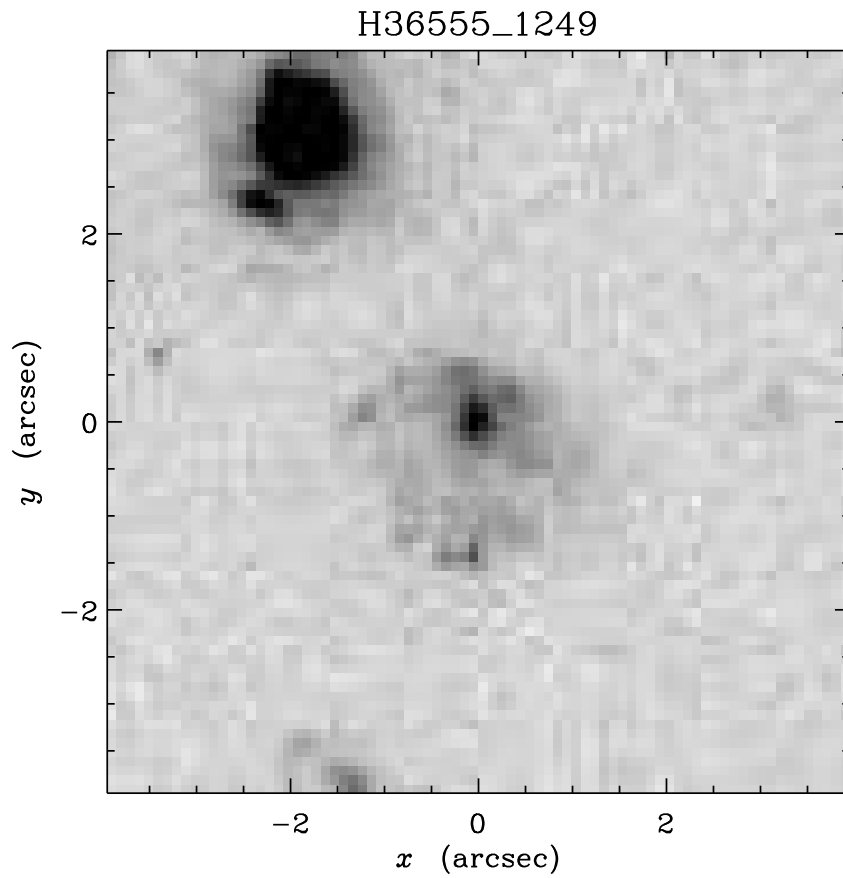


Fig. 7.— Probable proto-spiral at $z = 0.950$. Multi-color images show that the dense core of this object is red (old) and that the outer knots are blue (young).

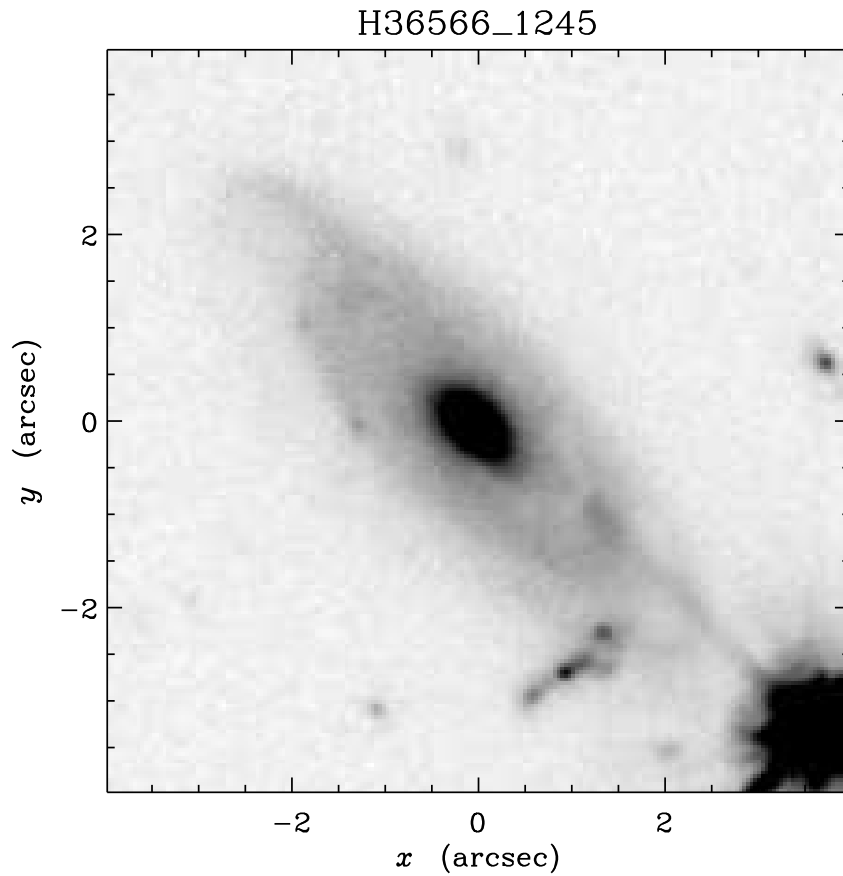


Fig. 8.— An Sb spiral at $z = 0.518$ which is peculiar because the spiral arms in the disk are underdeveloped compared to typical objects of similar type at $z \sim 0.0$. Note the multi-component (background) merger below and to the right of this object.

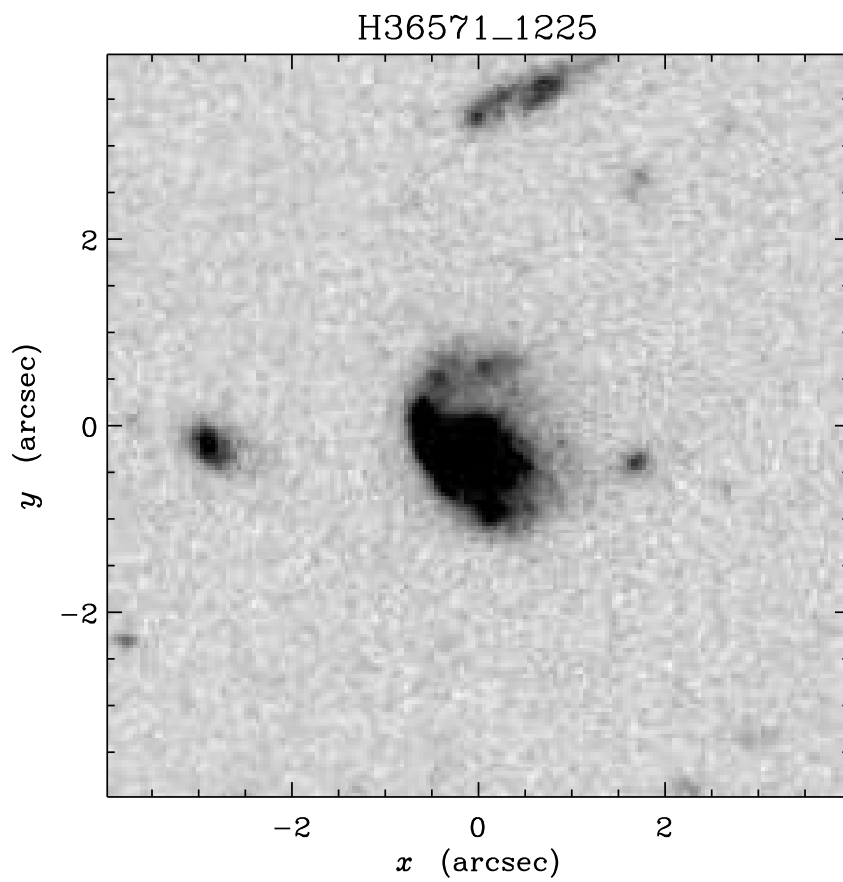


Fig. 9.— Note the malformed single spiral arm of this peculiar Sc galaxy at $z = 0.561$.

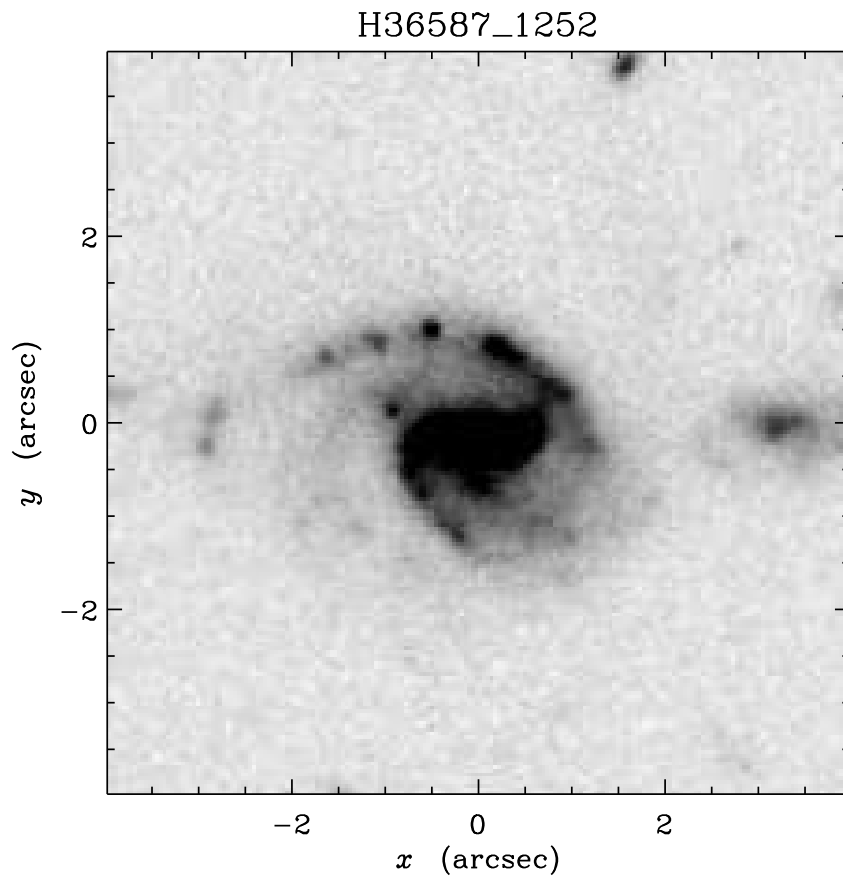


Fig. 10.— The most distant “certain” barred spiral in the present sample (at $z = 0.321$) is shown. Note the difference in the lengths of spiral arms in this SBc pec galaxy